Studying quarkonium in the anisotropic hot-dense quark-gluon plasma medium in the framework of generalized fractional derivative

M. Abu-Shady
Department of Mathematics and Computer Science, Faculty of Science, Menoufia University, Shbien El-Kom, Egypt.
e-mail: dr.abushady@gmail.com

Received 14 November 2022; accepted 27 February 2023

By applying the generalized fractional-Nikiforov-Uvarov approach, the radial Schrodinger equation is analytically solved in the longitudinal–traverse plane. The energy eigenvalues and associated functions are calculated by extending the interaction potential to an anisotropic hot-dense quark-gluon plasma medium. For heavy quarkonium masses like charmonium and bottomonium, the special cases of the mass of quarkonium are obtained at $\alpha = \beta = 1$. The effect of the fraction parameter is investigated within the context of the quark-gluon plasma medium on the binding energy and dissociation temperature when baryonic chemical potential is included. A comparison are studoed with recent works Therefore, the fractional quark model correctly represents heavy mesons in an anisotropic hot-dense quark-gluon plasma medium, according to the current findings.

Keywords: Generalized fractional derivative; Schrödinger equation; Nikiforov-Uvarov method; finite temperature; quarkonium spectra.

DOI: https://doi.org/10.31349/RevMexFis.69.040801

1. Introduction

It has been concluded from the ultra-relativistic heavy-ion collision experiments at RHIC and LHC that the quark-gluon plasma (QGP), which was created, behaves more like a perfect fluid than a non-interacting ultra-relativistic gas of quarks (anti-quarks) and gluons. The reason for this is because the QGP have a strong collective characteristic that may be measured in terms of the flow harmonics. In addition, the other significant signals based on experimental data, quarkonia suppression has also been proposed as a direct indicator of QGP creation in the collider studies. The tests show that it highlights the plasma properties of the medium, such as Landau damping, colour screening, and energy loss, see Ref. [1] and references therein.

At finite temperature, the evolution of the Schrodinger equation (SE) is vital. In order to study the creation of a hot quark-gluon plasma, Matsui and Satz [2] calculated the charmonium's J/Ψ radius. The properties of quarkonia in a thermal QCD medium in the background of strong magnetic field is studied using SE. Using a temperature-dependent potential deduced from lattice gauge computations. Wong [4] has investigated the binding energies and wave functions of heavy quarkonia in quark-gluon plasma. As a result, the study shows that the model with the modified Q-Q potential produces dissociation temperatures that are consistent with spectral function analyses. Also, the N-radial Schrodinger equation is analytically solved. The Cornell potential is extended to finite temperature and/or chemical potential as in Refs. [5-9] in which the energy eigenvalues and the wave functions are calculated.

A heavy quark potential at finite temperature was created by correctly introducing a dielectric function that encodes the effects of a deconfined medium to the full Cornell potential, not just its Coulomb part. This means that the heavy quark potential calculation has been expanded to include plasma with limited momentum-space anisotropy. For this case, specifically, the exact component has been calculated. As long as the quark-gluon plasma exhibits local momentum-space anisotropies for any finite shear viscosity, study of anisotropic plasma in the momentum space is necessary. These momentum-space anisotropies can continue for a very long period and can be rather significant depending on the strength of the shear viscosity, especially early on or close to the plasma's edges. This holds true for both strong and weak coupling shear viscosity levels, and increasing viscosity causes maximum momentum-space anisotropies to grow [10-14].

Recently, the fractional calculus has attracted attention in the different fields of physics. In high energy physics, the description of heavy-quarkonium energy spectra and complex phenomena of the standard model as in Ref. [15], in which, the author used the conformable fractional derivative to express the fractional radial SE in the N-dimensional space for the extended Cornell potential by using extended Nikiforov-Uvarov (ENU) method to the fractional domain. In Ref. [16] the fractional form of the NU method is applicable in order to solve fractional radial SE with its applications on variety of potentials such as the oscillator potential, Woods-Saxon potential, and Hulthen potential. The generalized fractional derivative [17,18] is suggested which is successfully applied in calculating quarkonium properties and molecular chemical properties as in Refs. [19-22].

The aim of the present work is to study the dissociation of quankonium in a hot-dense medium, in which the baryonic chemical potential is included in the framework of the generalized fractional derivative which are not considered in the recent works. The generalized fractional of the Nikiforov-Uvarov (CF-NU) method is applied to obtain the analytic solutions of the N-dimensional radial SE, then the results are applied on the investigation of binding energy and dissociation temperature.

The paper is organized as follows: In Sec. 2, the GF-NU method is briefly explained. In Sec. 3, The energy eigenvalue and wave function are calculated in the N-dimensional space using GF-NU method. In Sec. 4, the results are discussed. In Sec. 5, the summary and conclusion are presented.

2. The generalized fractional NU method

In this section, the GF-NU method is briefly given to solve the generalized fractional of differential equation which takes the following form (see Refs. [16,17,23], for details)

$$D^{\alpha}\left[D^{\alpha}\Psi(s)\right]+\frac{\bar{\tau}(s)}{\sigma(s)}D^{\alpha}\Psi(s)+\frac{\tilde{\sigma}(s)}{\sigma^{2}(s)}\Psi(s)=0, \quad (1)$$

where $\sigma(s)$ and $\tilde{\sigma}(s)$ are polynomials of maximum second degree of α and 2α, respectively and $\bar{\tau}(s)$ is a polynomial of maximum degree of α where

$$D^{\alpha}\Psi(s)=Is^{1-\alpha}\Psi'(s), \quad (2)$$

$$D^{\alpha}\left[D^{\alpha}\Psi(s)\right]=I^{2}\Bigg[(1-\alpha)\,s^{1-2\alpha}\Psi'(s) + s^{2-2\alpha}\Psi''(s)\Bigg]. \quad (3)$$

where

$$I=\frac{\Gamma(\beta)}{\Gamma(\beta-\alpha+1)}$$

where $0<\alpha\leq 1$and $0<\beta\leq 1$. Substituting by Eqs. 2) and (3) into (1), we obtain

$$\Psi''(s)+\frac{\bar{\tau}_{f}(s)}{\sigma_{f}(s)}\Psi'(s)+\frac{\tilde{\sigma}_{f}(s)}{\sigma_{f}^{2}(s)}\Psi(s)=0, \quad (4)$$

where, $\bar{\tau}_{f}(s) = (1-\alpha)\,s^{-\alpha}\sigma(s) + I^{-2}\bar{\tau}(s), \sigma_{f}(s) = s^{1-\alpha}\sigma(s), \tilde{\sigma}_{f}(s) = I^{-2}\tilde{\sigma}(s)$.To find the particular solution of Eq. (4) by separation of variables, if one deals with the transformation

$$\Psi(s)=\Phi(s)\chi(s), \quad (5)$$

it reduces to an equation of hypergeometric type as follows

$$\sigma_{f}(s)\chi''(s)+\tau_{f}(s)\chi'(s)+\lambda\chi(s)=0, \quad (6)$$

where

$$\sigma_{f}(s)=\pi_{f}(s)\frac{\Phi(s)}{\Phi'(s)}, \quad (7)$$

$$\tau_{f}(s)=\bar{\tau}_{f}(s)+2\pi_{f}(s);\quad \tau_{f}'(s)<0, \quad (8)$$

and

$$\lambda=\lambda_{n}=-n\tau_{f}'(s)-\frac{n(n-1)}{2}\sigma_{f}''(s), \quad n=0,1,2,... \quad (9)$$

$\chi(s)=\chi_{n}(s)$ which is a polynomial of n degree which satisfies the hypergeometric equation, taking the following form

$$\chi_{n}(s)=\frac{B_{n}}{\rho_{n}}\frac{d^{n}}{ds^{n}}(\sigma_{f}''(s)\rho(s)), \quad (10)$$

where B_n is a normalization constant and $\rho(s)$ is a weight function which satisfies the following equation

$$\frac{d}{ds}\omega(s)=\frac{\tau(s)}{\sigma_{f}(s)}\omega(s);\quad \omega(s)=\sigma_{f}(s)\rho(s), \quad (11)$$

$$\pi_{f}(s)=\frac{\sigma_{f}'(s)-\bar{\tau}_{f}(s)}{2} \pm\sqrt{\left(\frac{\sigma_{f}'(s)-\bar{\tau}_{f}(s)}{2}\right)^{2}-\tilde{\sigma}_{f}(s)+K\sigma_{f}(s)}, \quad (12)$$

and

$$\lambda=K+\pi_{f}'(s), \quad (13)$$

the $\pi_f(s)$ is a polynomial of first degree. The values of K in the square-root of Eq. (12) is possible to calculate if the expressions under the square root are square of expressions. This is possible if its discriminate is zero.

2.1. Real part of the potential in a anisotropic medium in the longitudinal–traverse plane

Here, we aim to find the potential due to the presence of a dissipative anisotropic hot QCD medium. The in-medium modification can be obtained in the Fourier space by dividing the heavy-quark potential by the medium dielectric permittivity, $\epsilon(K)$ as follows

$$\tilde{V}(k)=\frac{V(k)}{\epsilon(K)}, \quad (14)$$

by taking the inverse Fourier transform, the the modified potential is obtained as follows

$$V(r)=\int\frac{d^{3}k}{(2\pi)^{\frac{3}{2}}}\left(e^{ik\cdot r}-1\right)\tilde{V}(k), \quad (15)$$

where $V(k)$ is the Fourier transform of Cornell potential $V(r)=(-\alpha_1/r)+\sigma r$ that gives as follows

$$V(k)=-\sqrt{\frac{2}{\pi}}\left(\frac{\alpha_{1}}{k^{2}}+\frac{2\sigma}{k^{4}}\right), \quad (16)$$

where $\epsilon(K)$ may be calculated which found from the self-energy using finite temperature QCD. By applying hard thermal loop resummation technique as in Refs. [25,26], the static gluon propagator which represents the inelastic scattering of an off-shell gluon to a thermal gluon is defined as follows

$$\Delta^{\mu\nu}(w,k)=k^2g^{\mu\nu}-k^\mu k^\nu+\Pi^{\mu\nu}(w,k), \tag{17}$$

the dielectric tensor can then be obtained in the static limit in Fourier space, from the temporal component of the propagator as

$$\epsilon^{-1}(K)=-\lim_{w\to 0}k^2\Delta^{00}(w,k). \tag{18}$$

To calculate the real part of the inter-quark potential in the static limit, one can obtain first the temporal component of real part of the retarded propagator in Fourier space at finite temperature and chemical potential as follows

$$\mathrm{Re}\left[\Delta_R^{00}\right](w=0,k)=-\frac{1}{k^2+m_D^2(T,\mu)}-\xi\left(\frac{1}{3\left(k^2+m_D^2(T,\mu)\right)}\right)-\frac{m_D^2(T,\mu)\left(3\cos 2\theta-1\right)}{6\left(k^2+m_D^2(T,\mu)\right)^2}, \tag{19}$$

where the medium dielectric permittivity $\epsilon(K)$ is then given by

$$\epsilon^{-1}(K)=\frac{k^2}{k^2+m_D^2}+k^2\xi\left(\frac{1}{3\left(k^2+m_D^2\right)}\right)-\frac{m_D^2\left(3\cos 2\theta-1\right)}{6\left(k^2+m_D^2\right)^2} \tag{20}$$

Substituting Eqs. (22) and (18) into Eq. (16) and then taking its inverse Fourier transform, we can write the real part of the potential for $rm_D\ll 1$ as

$$V(r,\xi,T,\mu_b)=\sigma r\left(1+\frac{\xi}{3}\right)-\frac{\alpha_1}{r}\left(1+\frac{(rm_D)^2}{2}+\xi\left(\frac{1}{3}+\frac{(rm_D)^2}{16}\left(\frac{1}{3}+\frac{(rm_D)^2}{16}\left(\frac{1}{3}+\cos(2\theta)\right)\right)\right)\right), \tag{21}$$

where ξ is the anisotropic parameter, and T and μ_b are the temperature and the baryonic chemical potential, respectively. In Eq. (21), we note that the potential reduces to the Cornell potential for $\xi=0$ and $m_D=0$ (For details, see Ref. [25]). In the present work, the Debye mass $D(T,\mu_b)$ is given as in Refs. [27,28] by

$$D(T,\mu_b)=gT\sqrt{\frac{N_c}{3}+\frac{N_f}{6}+\frac{N_f}{2\pi^2}\left(\frac{\mu_q}{T}\right)^2}, \tag{22}$$

where, g is the coupling constant as defined in Ref. [29], μ_q is the quark chemical potential ($\mu_q=\mu_b/3$), N_f is number of flavours, and N_c is number of colours. The potential depends on θ which is the angle between the particle momentum and the direction of anisotropy.

2.2. The particle momentum is longitudinal the direction of anisotropy

For r parallel to the direction of n of anisotropy at $\theta=0$, The potential is given by

$$V(r)=a_1r-\frac{b_1}{r}, \tag{23}$$

where

$$a_1=\sigma+\frac{1}{3}\sigma\xi-\frac{1}{2}\alpha_1m_D^2-\frac{1}{48}\alpha_1\xi m_D^2, \tag{24}$$

$$b_1=\alpha+\frac{\alpha\xi}{3}. \tag{25}$$

It is important to mention in Eq. (23) that we have not observed any anisotropy in the present potential. This can be understood physically: The tensorial (nonsphericity) nature of the potential in the coordinate space arises due to anisotropy in the momentum space. However, we are restricted to a plasma which is very much close to equilibrium because that $\xi\leq 1$, by the time quarkonium states are formed in the plasma around $(1-2)\,T_c$, the plasma becomes almost isotropized at θ parallel to n. In addition, recently a novel magnetic field-induced anisotropic behavior was first observed in the heavy quark potential in the longitudinal–traverse plane with respect to the direction of B, in which the radial Shrödinger equation with anisotropic potential is solved on the two cases as in Refs. [3,13].

2.3. The particle momentum is perpendicular to the direction of anisotropy

For r perpendicular to the direction of n of anisotropy at $\theta=\pi/2$, the potential in Eq. (23) is simplified into

$$V(r)=a_2r-\frac{b_1}{r}, \tag{26}$$

where

$$a_2=\sigma+\frac{1}{3}\sigma\xi-\frac{1}{2}\alpha_1m_D^2+\frac{1}{24}\alpha_1\xi m_D^2.$$

3. The Generalized Fractional of Schrödinger Equation

In this section, the SE is solved in the longitudinal–traverse plane as in Refs. [3,13] and references therein so, the SE for two particles interacting via the potential $V(r,\xi)$ in the N-dimensional space, where r is inter-particle distance, is given by [24]

$$\left[\frac{d^2}{dr^2}+\frac{(N-1)}{r}\frac{d}{dr}-\frac{L(L+N-2)}{r^2}+2\mu(E-V\left(r,\xi\right)\right]\Psi(r)=0, \tag{27}$$

where $L, N,$ and μ are the angular momentum quantum number, the dimensionality number and the reduced mass for the quarkonium particle (for charmonium $\mu = m_c/2$ and for bottomonium $\mu = m_b/2$), respectively. Setting the wave function $\Psi(r) = R(r)r^{(1-N/2)}$, the following radial SE is obtained

$$\left[\frac{d^2}{dr^2}+2\mu\left(E-V\left(r,\xi\right)-\frac{(L+\frac{(N-2)}{2})^2-\frac{1}{4}}{2\mu r^2}\right)\right]R(r)=0, \tag{28}$$

where $V\left(r,\xi\right)$ is the interaction potential given in Eq. (23). By substituting by Eq. (23) into Eq. (28), we obtain

$$\left[\frac{d^2}{dr^2}+2\mu\left(E+\frac{b_1}{r}-a_1 r-\frac{(L+\frac{(N-2)}{2})^2-\frac{1}{4}}{2\mu r^2}\right)\right]R(r)=0. \tag{29}$$

By taking $r = 1/x$, Eq. (29) takes the following form

$$\left[\frac{d^2}{dx^2}+\frac{2x}{x^2}\frac{d}{dx}+\frac{2\mu}{x^4}\left(E+b_1 x-\frac{a_1}{x}-\frac{(L+\frac{(N-2)}{2})^2-\frac{1}{4}}{2\mu}x^2\right)\right]R(x)=0. \tag{30}$$

The expansion of a_1/x in a power series around the characteristic radius r_0 of meson up to the second order is used as in Ref. [13]. The following equation is obtained

$$\left[\frac{d^2}{dx^2}+\frac{2x}{x^2}\frac{d}{dx}+\frac{2}{x^4}(-D_1+D_2 x-D_3 x^2)\right]R(x)=0, \tag{31}$$

where,

$$D_1=-\mu\left(E-\frac{3a_1}{\delta}\right),\quad D_2=\mu\left(\frac{3a_1}{\delta^2}+b_1\right),\quad \text{and}\quad D_3=\mu\left(\frac{a_1}{\delta^3}+\frac{(L+\frac{(N-2)}{2})^2-\frac{1}{4}}{2\mu}\right). \tag{32}$$

To transform Eq. (31) into a fractional form, one uses dimensionless form by taking $y = Ax$ where A equals 1 GeV.

$$\left[\frac{d^2}{dy^2}+\frac{2y}{y^2}\frac{d}{dy}+\frac{2}{y^4}(-D_{11}+D_{22}y-D_3 y^2)\right]R(y)=0, \tag{33}$$

where

$$D_{11}=\frac{D_1}{A^2},\quad D_{22}=\frac{D_2}{A}. \tag{34}$$

By using Refs. [16,17] one can put Eq. (33) in the following form:

$$\left[D^\alpha\left[D^\alpha R(y)\right]+\frac{2y^\alpha}{y^{2\alpha}}D^\alpha R(y)+\frac{2}{y^{4\alpha}}(-D_{11}+D_{22}y^\alpha-D_3 y^{2\alpha})\right]R(y)=0, \tag{35}$$

and substituting Eqs. (2) and (3) into (35), we obtain

$$R''(y)+\frac{\bar{\tau}_f(y)}{\sigma_f(y)}R'(x)+\frac{\tilde{\sigma}_f(y)}{\sigma_f^2(y)}R(y)=0, \tag{36}$$

where

$$\bar{\tau}_f(s)=(1-\alpha)\,y^\alpha+2I^{-2}y^\alpha,\sigma_f(s)=y^{\alpha+1},\text{and }\tilde{\sigma}_f(y)=2I^{-2}(-D_1+D_2y^\alpha-D_3y^{2\alpha}). \tag{37}$$

Hence, the Eq. (36) satisfies Eq. (4). Therefore, Eq. (12) takes the following form after substituting by Eq. (37),

$$\pi_f=-y^\alpha+\alpha I^{-2}y^\alpha\pm\sqrt{\left(-y^\alpha+\alpha I^{-2}y^\alpha\right)^2-2I^{-2}(-D_{11}+D_{22}y^\alpha-D_3y^{2\alpha})+Ky^{1+\alpha}}. \tag{38}$$

The constant K is chosen such as the function under the square root has a double zero, *i.e.*, its discriminant equals zero. Hence,

$$K=\left(\frac{I^{-2}D_{22}^{2}}{2D_{11}}-(1-2\alpha I^{-2}+\alpha^{2}I^{-4}+2I^{-2}D_{3})\right)y^{\alpha-1}. \tag{39}$$

Substituting by Eq. (39) into Eq. (38), we obtain

$$\pi_{f}\left(y\right)=-y^{\alpha}+\alpha I^{-2}y^{\alpha}+\frac{D_{22}}{\sqrt{2D_{11}}}y^{\alpha}-\sqrt{2D_{11}} \tag{40}$$

The positive sign in Eq. (38) is determined as in Ref. [15]. By using Eq. (8), we obtain

$$\tau_{f}(y)=\left(1-\alpha\right)y^{\alpha}+2y^{\alpha}-2\left(\frac{D_{22}}{\sqrt{2D_{11}}}y^{\alpha}-\sqrt{2D_{11}}\right), \tag{41}$$

and using Eq. (14), we obtain

$$\lambda_{n}=\left(-n\left(3\alpha-\alpha^{2}\right)-\frac{2nD_{22}\alpha}{\sqrt{2D_{11}}}-\frac{n\left(n-1\right)\alpha\left(\alpha+1\right)}{2}\right)y^{\alpha-1}. \tag{42}$$

From Eq. (9), $\lambda=\lambda_{n}$. The energy eigenvalues of Eq. (36) in the N-dimensional space are

$$E_{nL}^{N}=\frac{3a_{1}}{\delta}-\frac{2\mu I^{-4}(\frac{3a_{1}}{\delta^{2}}+b_{1})^{2}}{[(2n+1)\,\alpha+\sqrt{\left(2n+1\right)^{2}\alpha^{2}-4I^{-2}W}]^{2}}. \tag{43}$$

with

$$W=n\left(3\alpha-\alpha^{2}\right)+\frac{1}{2}n\left(n-1\right)\alpha\left(\alpha+1\right)-(1-2\alpha I^{-2}+\alpha^{2}I^{-4}+2I^{-2}D_{3})-\alpha+\alpha^{2}I^{-2}. \tag{44}$$

The radial of wave function takes the following form

$$R_{nL}\left(r^{\alpha}\right)=C_{nL}\,r^{\left(-\frac{D_{2}}{\sqrt{2D_{1}}}-1\right)\alpha}e^{\sqrt{2D_{1}}r^{\alpha}}(-r^{2\alpha}D^{\alpha})^{n}\left(r^{\left(-2n+\frac{D_{2}}{\sqrt{2D_{1}}}\right)\alpha}e^{-2\sqrt{2D_{1}}r^{\alpha}}\right), \tag{45}$$

where C_{nL} is the normalization constant that is determined by $\int\left|R_{nL}\left(r^{\alpha}\right)\right|^{2}dr=1$. We note that the radial wave function in Eq. (45) does not explicitly depend on the number of dimensions. Hence, $\int\left|R_{nL}\left(r\right)\right|^{2}dr=1$ remains unchanged.

4. Discussion of results

In this section, the above results are applied to the quarkonium masses. The quarkonium mass considering fraction-order and dimensionality in the hot-dense medium is [29]

$$M=2m+E_{nL}^{N}, \tag{46}$$

$$M=2m+\frac{3a_{1}}{\delta}-\frac{2\mu I^{-4}(\frac{3a_{1}}{\delta^{2}}+b_{1})^{2}}{[(2n+1)\,\alpha+\sqrt{\left(2n+1\right)^{2}\alpha^{2}-4I^{-2}W}]^{2}}, \tag{47}$$

where m is quarkonium bare mass for the charmonium or bottomonium mesons. By using Eq. (42), we write Eq. (45) as in Eq. (46). One can obtain the quarkonium masses at zero temperature by taking $T=\mu_{b}=\xi=0\Rightarrow D(T,\mu_{b})$ at $\alpha=\beta=1$ and $N=3$. Therefore, Eq. (46) takes the following form

$$M_{Q}=2m+\frac{3\sigma}{\delta}-\frac{2\mu(\frac{3\sigma}{\delta^{2}}+\alpha)^{2}}{[(2n+1)+\sqrt{1+\frac{8\mu\sigma}{\delta^{3}}+4L(L+1)}]^{2}}. \tag{48}$$

Eq. (47) coincides with Ref. [30], in which the authors obtained the quarkonium mass at zero temperature and $\alpha=\beta=1$ at $N=3$.

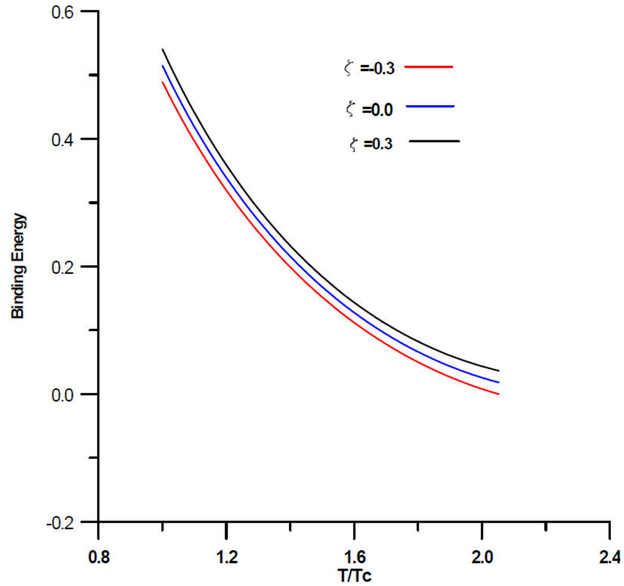

FIGURE 1. The binding energy of 1S state for $C\bar{C}$ is plotted as a function of ratio tempearture for different values of ζ at $u_b = 0.3$ GeV in the fractional model $\alpha = \beta = 1/2$.

In the present analysis, various quantities have been obtained, and the results are plotted while considering the weak anisotropy in the hot QCD plasma with the fixed critical temperature $T_c = 0.17$ GeV. We considered $\zeta = -0.3$ for prolate and $\zeta = 0.3$ for oblate, whereas for the isotropic case, we have $\zeta = 0$. As discussed earlier, the dissociation temperature has been obtained by employing the following criterion: The temperature at which the binding energy equals and causes dissociation of quarkonia is the dissociation temperature [25]. In Fig. 1, we note that the binding

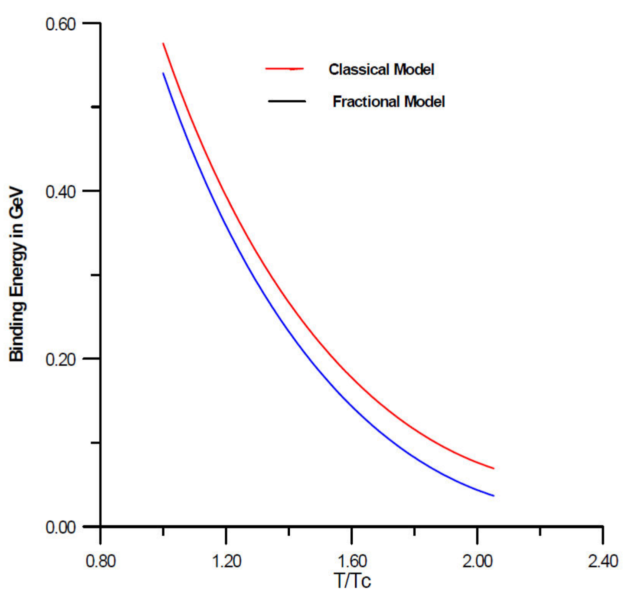

FIGURE 2. The binding energy of 1S state for $C\bar{C}$ is plotted as a function of ratio tempearture for the classical model at $\alpha = \beta = 1$ and the fractional model $\alpha = \beta = 1/2$ at $u_b = 0.3$ GeV and $\zeta = 0.3$.

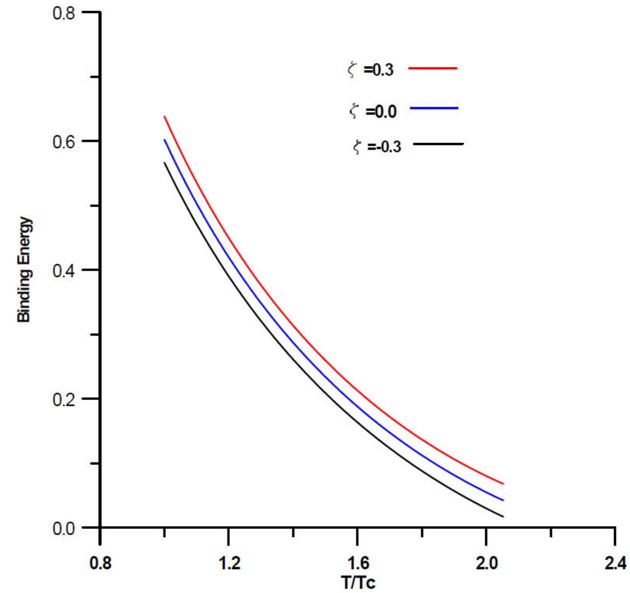

FIGURE 3. The binding energy of 1S state for $b\bar{b}$ state is plotted as a function of ratio tempearture for different values of ζ at $u_b = 0.3$ GeV in the fractional model at $\alpha = \beta = 1/2$.

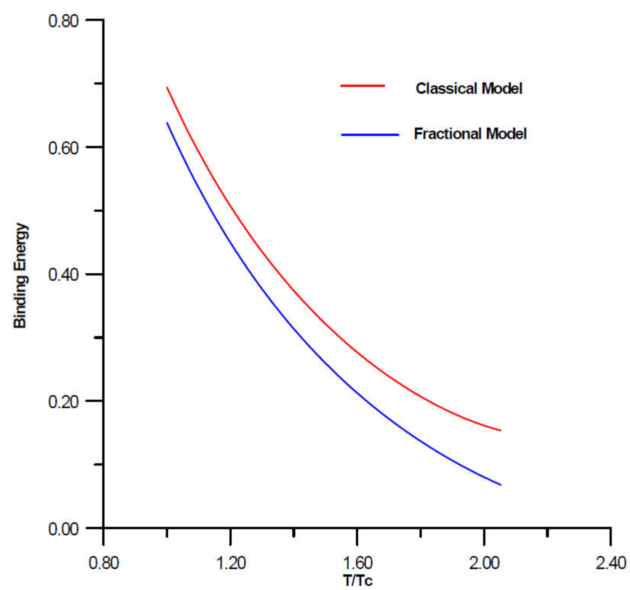

FIGURE 4. The binding energy of 1S state for $b\bar{b}$ is plotted as a function of ratio tempearture for the classical model at $\alpha = \beta = 1$ and the fractional model $\alpha = \beta = 1/2$ at $u_b = 0.3$ GeV and $\zeta = 0.3$.

energy $(E_b = V(r \to \infty) - E_{nl})$ decreases with increasing temperature at finite baryonic chemical potential $(u_b = 0.3\ \text{GeV})$ and $\alpha = \beta = 0.5$. In addition, the curves shift to upper values by increasing anisotropic parameter ζ that is agreement with Ref. [1], in which authors investigated the behavior of binding energy in the hot medium without including baryonic potential. In Fig. 2, a comparison between the classical model at $\alpha = \beta = 1$ and the fractional model at $\alpha = \beta = 0.5$, we note that the binding energy takes a similar

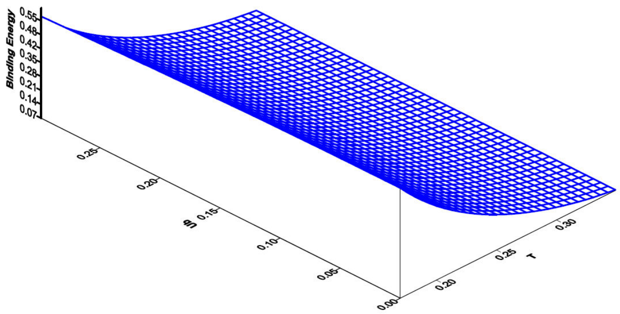

FIGURE 5. The binding energy of 1S state for $C\overline{C}$ is plotted as a function of T and u_b at $\alpha = \beta = 1$ and $\zeta = 0.3$.

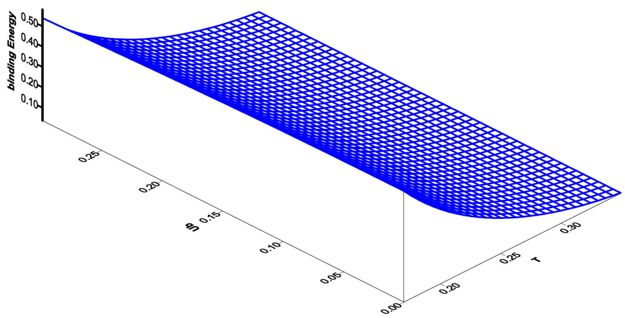

FIGURE 6. The binding energy of 1S state for $C\overline{C}$ is plotted as a function of T and u_b at $\alpha = \beta = 0.5$ and $\zeta = 0.3$.

behavior in which the binding energy decreases with increasing temperature. Also in the fractional model, we note that the binding energy shifts to lower values and thus, the fractional parameter will be affected on the dissociation temperature in hot-dense medium. A similar situation takes place for bottominum energy in the fractional model at $\alpha = \beta = 0.5$ and in the classical model at $\alpha = \beta = 1$ as in Figs. 3 and 4.. In Fig. 5, the binding energy for charmonium is plotted in 3D as a function of temperature and baryonic chemical potential in the classical model at $\alpha = \beta = 1$. We note that the effect of temperature on the binding temperature is more affected in comparison with the effect of baryonic chemical potential. We note that the binding energy decreases slightly by increasing baryonic chemical potential. A similar situation is obtained in the fractional model at $\alpha = \beta = 0.5$ but we note that the binding has a smaller values. In Figs. 7 and 8 the

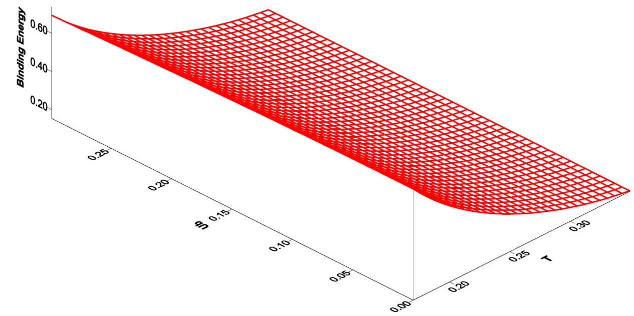

FIGURE 7. The binding energy of 1S state for $b\overline{b}$ is plotted as a function of T and u_b at $\alpha = \beta = 1$ and $\zeta = 0.3$.

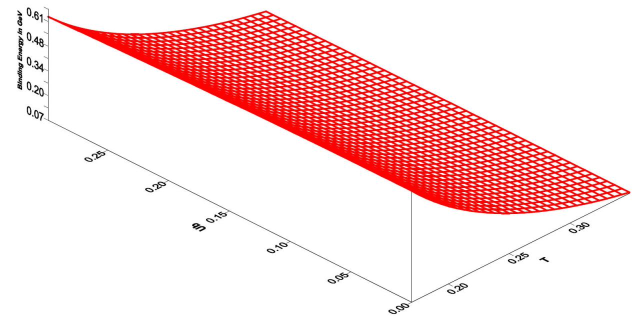

FIGURE 8. The binding energy of 1S state for $b\overline{b}$ is plotted as a function of T and u_b at $\alpha = \beta = 0.5$ and $\zeta = 0.3$.

binding energy of bottomonium is plotted in 3D. We note that the temperature is more effect on the binding energy than the baryonic chemical potential in the classical fractional model.

The dissociation temperature for both the classical model and the fractional model is shown in Tables I and II.

For the 1S and 2S of charmonium and bottominum, we observe that the dissociation temperature increases as the anisotropic parameter increases. Additionally, we observe that 2S state has smaller values than those in the 1S state. The fractional model is used for obtaining the results in Table II to compute the dissociation temperature at $\alpha = \beta = 0.5$. We see in Figs. 2 and 4 that the fractional parameter decreases the binding energy cause the dissociation temperature is lower than the classical model at $\alpha = \beta = 1$. This result is qualitatively consistent with Ref. [1], where the authors used another technique to determine the dissociation temperature by the temperature at which twice the binding energy (real part) equals the thermal width. Additionally, the results of the fractional model qualitatively agree with those of Ref. [25], in which the authors determined the dissociation temperature by the temperature at which it equals the real part of the binding energy, leading quarkonia to dissociate.

TABLE I. The dissociation temperature for charmonium and bottominum states in units of T_c at $\alpha = \beta = 1$.

$c\bar{c}$	1S	2S	$b\bar{b}$	1S	2S
$\zeta = 0.3$	1.465	1.424	$\zeta = 0.3$	1.629	1.547
$\zeta = 0.0$	1.435	1.400	$\zeta = 0.0$	1.576	1.524
$\zeta = -0.3$	1.376	1.376	$\zeta = -0.3$	1.518	1.488

TABLE II. The dissociation temperature for charmonium and bottominum states in units of T_c at $\alpha = \beta = 0.5$.

$c\bar{c}$	1S	2S	$b\bar{b}$	1S	2S
$\zeta = 0.3$	1.418	1.411	$\zeta = 0.3$	1.529	1.511
$\zeta = 0.0$	1.394	1.388	$\zeta = 0.0$	1.494	1.482
$\zeta = -0.3$	1.371	1.364	$\zeta = -0.3$	1.459	1.447

5. Summary and Conclusion

In this study, we examined the binding energy and dissociation temperature in the fractional nonrelativistic model (FNM). The NU technique is analytically used to solve the FNM. The fractional model of the eigenvalues of the energy and wave functions is obtained. As a result, we determined the special cases that were consistent with the classical model. Additionally, we soon realize that the fractional form's binding energy is lower than it was in the classical model; as a result, the dissociation temperature in a hot-dense medium decreases in comparison to the classical model. We found the dissociation temperature was agreement with other studies, such as Ref. [25]. Also, we note that the effect of baryonic chemical potential is slightly less pronounced on binding energy. This finding is not considered in other works in the framework of the fractional model. In addition, the excited states are obtained for charmonium and bottominum.

Finally, we found that the fate of heavy-quarkonia states in the hot-dense QCD medium is significantly influenced by both the anisotropy and the hot-dense QCD medium effects present in EoS when fractional calculus is taken into account.

---

1. J. Mohammad Yousuf, *et al*., Dissociation of heavy quarkonia in an anisotropic hot QCD medium in a quasiparticle model. *Physical Review D* **97** (2018) 094033, `https://doi.org/10.1103/PhysRevD.97.094033`.
2. T. Matsui, and H. Satz, J/Ψ suppression by quark-gluon plasma formation. *Physics Letters B*, **178** (1986) 416, `https://doi.org/10.1016/0370-2693(86)91404-8`.
3. M. Hasan, B. Chatterjee, and B. K. Patra, Heavy Quark Potential in a static and strong homogeneous magnetic field, *Eur. Phys. J C* **77** (2017) 767, `https://doi.org/10.1140/epjc/s10052-017-5346-z`.
4. C. Y. Wong, Dissociation of a heavy quarkonium at high temperatures. *Phys. Rev. C*, **65** (2002) 034902, `https://doi.org/10.1103/PhysRevC.65.034902`.
5. M. Abu-Shady, N-dimensional Schrodinger equation at finite temperature using the Nikiforov–Uvarov method. *J. Egypt. Math. Soc.* **25** (2017) 86-89.
6. M. Abu-Shady, and A. N. Ikot. Analytic solution of multi-dimensional Schrodinger equation in hot and dense QCD media using the SUSYQM method. *Eur. Phys. J. Plus* **134** (2019) 321, `https://doi.org/10.1140/epjp/i2019-12685-y`.
7. M. Abu-Shady, C. O. Edet, and A. N. Ikot, Non-relativistic quark model under external magnetic and Aharanov–Bohm (AB) fields in the presence of temperature-dependent confined Cornell potential. *Can. J. Phys.* **99** (2021) 1024, `https://doi.org/10.1139/cjp-2020-0101`.
8. M. Abu-Shady, T. A. Abdel-Karim, and E. M. Khokha, Binding Energies and Dissociation Temperatures of Heavy Quarkonia at Finite Temperature and Chemical Potential in the-Dimensional Space. *Adv. High Energy Phys*. **2018** (2018) 7356843, `https://doi.org/10.1155/2018/7356843`.
9. M. Abu-Shady, Multidimensional Schrödinger Equation and Spectral Properties of Heavy-Quarkonium Mesons at Finite Temperature. *Adv. Math. Phys.* **2016** (2016) 4935940, `https://doi.org/10.1155/2016/4935940`.
10. A. Dumitru, Y. Guo, A. Mocsy, and M. Strickland, *Phys. Rev. D* **79** (2009) 054019, `https://doi.org/10.1103/PhysRevD.79.054019`.
11. A. Dumitru, Y. Guo, and M. Strickland, The Heavy-quark potential in an anisotropic (viscous) plasma, *Phys. Lett. B* **662** (2008) 37, `https://doi.org/10.1016/j.physletb.2008.02.048`.
12. R. Ryblewski and W. Florkowski, Non-boost-invariant motion of dissipative and highly anisotropic fluid, *J. Phys. G* **38** (2011) 015104, `https://doi.org/10.1088/0954-3899/38/1/015104`.
13. M. Abu-Shady, and H. M. Fath-Allah. Melting of quarkonium in an anisotropic hot QCD medium in the presence of a generalized Debye screening mass and Nikiforov–Uvarov's method. *Int. J. Mod. Phys. A* **35** (2020) 2050110, `https://doi.org/10.1142/S0217751X20501109`.
14. M. Abu-Shady, H. M. Mansour, and A. I. Ahmadov. Dissociation of quarkonium in hot and dense media in an anisotropic plasma in the nonrelativistic quark model. *Adv. High Energy Phys.* **2019** (2019) 4785615, `https://doi.org/10.1155/2019/4785615`.
15. Al-Jamel, Ahmed, The search for fractional order in heavy quarkonia spectra. *Int. J. Mod. Phys. A* **34** (2019) 1950054, `https://doi.org/10.1142/S0217751X19500544`.
16. H. Karayer, D. Demirhan and F. Büyükkılıç, Conformable Fractional Nikiforov-Uvarov Method, *Commun. Theor. Phys*. **66** (2018) 12, `https://doi.org/10.1088/0253-6102/66/1/012`.

17. M. Abu-Shady and M. K. A. Kaabar, A generalized definition of the fractional derivative with applications, *Math. Probl. Eng.* **2021** (2021) 9444803, https://doi.org/10.1155/2021/9444803.

18. M. Abu-Shady, and M. K. A. Kaabar. A novel computational tool for the fractional-order special functions arising from modeling scientific phenomena via Abu-Shady–Kaabar fractional derivative. *Comput. Math. Methods Medicine* **2022** (2022) 2138775, https://doi.org/10.1155/2022/2138775.

19. M. Abu-Shady, E. M. Khokha, and T.A. Abdel-Karim, The generalized fractional NU method for the diatomic molecules in the Deng–Fan model. *Eur. Phys. J. D* **76** (2022) 159, https://doi.org/10.1140/epjd/s10053-022-00480-w.

20. M. Abu-Shady, A. I. Ahmado, H. M. Fath-Allah and V. H. Badalov, Spectra of heavy quarkonia in a magnetized-hot medium in the framework of fractional non-relativistic quark model, *J. Theo. and App. Phys.* **16** (2022) 162225, https://doi.org/10.30495/jtap.162225.

21. M. Abu-Shady and E. P. Inyang, Heavy-Meson Masses in the Framework of Trigonometric Rosen-Morse Potential Using the Generalized Fractional Derivative, *East Eur. J. Phys.* **2022** (2022) 80, https://doi.org/10.26565/2312-4334-2022-4-06.

22. M. Abu-shady, H. M. Fath-Allah, Masses of Single, Double, and Triple Heavy Baryons in the Hyper-Central Quark Model by Using GF-AEIM, *Adv. High Energy Phys.* **2022** (2022) 4539308, https://doi.org/10.1155/2022/4539308.

23. A. F. Nikiforov and V. B. Uvarov, Special Functions of Mathematical Physics, (Birkh$\ddot{a}$user, Basel 1988).

24. M. Abu-Shady, and E. M. Khokha, Heavy-light mesons in the nonrelativistic quark model using Laplace transformation method, *Adv. High Energy Phys*. **2018** (2018) 7032041, https://doi.org/10.1155/2018/7032041.

25. L. Thakur, N. Haque, U. Kakade, and B. K. Patra, Dissociation of quarkonium in an anisotropic hot QCD medium. *Phys. Rev. D,* **88** (2013) 054022, https://doi.org/10.1103/PhysRevD.88.054022.

26. O. Kaczmarek, Screening at finite temperature and density, hep-let/07100498 (2007).

27. M. Moring, S. Ejir, O. Kaczmarek, F. Karsch and E. Laermann, PoSLAT **2005** (2006) 193, https://doi.org/10.22323/1.020.0193.

28. B. Liu, Shen, P. N., and Chiang, H. C. Heavy quarkonium spectra and J/Ψ dissociation in hot and dense matter. *Phys. Rev. C.* **55** (1997) 3021, https://doi.org/10.1103/PhysRevC.55.3021.

29. M. Abu-Shady, and Sh Y. Ezz-Alarab, Trigonometric Rosen-Morse potential as a quark-antiquark interaction potential for meson properties in the nonrelativistic quark model using EAIM, *Few Body Syst*. **60** (2019) 66, https://doi.org/10.1007/s00601-019-1531-y.

30. M. Abu-Shady, Heavy Quarkonia and $b\bar{c}$-Mesons in the Cornell Potential with Harmonic Oscillator Potential in the N-dimensional SchrÃ¶dinger Equation, *Int. J. Appl. Math. Theor. Phys.* **2** (2016) 16, https://doi.org/10.11648/j.ijamtp.20160202.11.